

Final Report

**STUDY OF THE BREAKDOWN CHARACTERISTICS OF ANTENNAS
IN THE ATMOSPHERES OF MARS AND VENUS**

Prepared for:

JET PROPULSION LABORATORY
4800 OAK GROVE DRIVE
PASADENA, CALIFORNIA

CONTRACT 950380
UNDER NASA CONTRACT NAS 7-100

By: J. A. Martin J. Chown

STANFORD RESEARCH INSTITUTE

MENLO PARK, CALIFORNIA

***SRI**

FACILITY FORM 802

N64-33094	
(ACCESSION NUMBER)	(THRU)
30	1
(PAGES)	(CODE)
NASA CR 59111	08
(NASA CR OR TMX OR AD NUMBER)	(CATEGORY)

OTS PRICE

XEROX	\$	2.00
MICROFILM	\$.50



February 1963

Final Report

**STUDY OF THE BREAKDOWN CHARACTERISTICS OF ANTENNAS
IN THE ATMOSPHERES OF MARS AND VENUS**

Prepared for:

JET PROPULSION LABORATORY
4800 OAK GROVE DRIVE
PASADENA, CALIFORNIA

CONTRACT 950380
UNDER NASA CONTRACT NAS 7-100

By: J. A. Martin J. Chown

SRI Project No. 4208

Approved:

T. MORITA, MANAGER ELECTROMAGNETIC SCIENCES LABORATORY

D. R. SCHEUCH, DIRECTOR ELECTRONICS AND RADIO SCIENCES DIVISION

Copy No. 1

ABSTRACT

33094

The objective of this study was to determine the power-handling capability and breakdown-power level of several typical linear and circularly polarized antennas in the simulated atmospheres of Mars and Venus. For the N_2 , CO_2 , and Ar concentrations forming the simulated atmospheres employed here, the breakdown power level of the antennas was not significantly different from that experienced in air.

Measured power required to initiate breakdown of 0.26λ cylindrical monopole antennas is presented for $\Omega = 13.8, 12.0, 10.6, 10.1, 9.2, 7.8, 6.0$, and 5.0 [$\Omega = 2 \ln (4 \text{ length/dia})$ of antenna]. Measured breakdown power as a function of pressure is presented also for a cylindrical dipole antenna. The antenna scaling principle was verified at frequencies of 250 Mc (CW), 1197 Mc (pulse) and 3000 Mc (pulse), using monopole antennas of different thickness ratio, Ω .

The tip field was measured on several cylindrical quarter-wave monopoles using a small probe. A curve relating the tip field required for tip breakdown is presented, providing a means of predicting breakdown levels.

Author

CONTENTS

ABSTRACT.	ii
LIST OF ILLUSTRATIONS	iv
LIST OF TABLES.	v
I INTRODUCTION	1
II CYLINDRICAL MONOPOLE BREAKDOWN	2
A. Breakdown in Air	2
B. Verification of Antenna Scaling Principle.	4
C. Breakdown Field Measurements	9
D. Breakdown in Simulated Atmospheres of Mars and Venus . .	11
III CROSS-DIPOLE ANTENNA BREAKDOWN	15
IV HELICAL ANTENNA BREAKDOWN.	17
V CONCLUSIONS.	21
REFERENCES.	22
ACKNOWLEDGEMENTS.	23

ILLUSTRATIONS

Fig. 1	Monopole Antennas	3
Fig. 2	Power Required to Initiate Breakdown in Air of 0.26λ Monopoles as a Function of Pressure and Frequency	4
Fig. 3	Power Required to Initiate Breakdown in Air of 0.26λ Monopoles as a Function of Diameter and Frequency for $p/f = 8 \times 10^{-4}$ mm Hg/ megacycles.	5
Fig. 4	Power Required to Initiate Breakdown in Air of 0.26λ Monopoles as a Function of Ω and ℓ/d for $p/f = 8 \times 10^{-4}$ mm Hg/megacycles	6
Fig. 5	Verification of Antenna Scaling Principle and Breakdown for $\Omega = 7.8$ Monopoles as a Function of Pressure and Frequency.	7
Fig. 6	Verification of Antenna Scaling Principle and Breakdown for $\Omega = 5.0$ Monopoles as a Function of Pressure and Frequency.	8
Fig. 7	Average Value of Normalized Breakdown Parameters for CW Breakdown of Monopole Antennas.	10
Fig. 8	Gas Mixing Equipment.	13
Fig. 9	Measured Values of Power to Initiate CW Breakdown of a $\Omega = 7.8$ Monopole in Simulated Atmospheres of Mars and Venus	14
Fig. 10	Power Required to Initiate Breakdown in Air of a Crossed-Dipole Antenna	16
Fig. 11	L-Band 6-Turn Helical Antenna in Plexiglas Chamber	18
Fig. 12	Power Required to Initiate Breakdown in Air of 6-Turn Axial-Mode Helical Antenna.	19
Fig. 13	Helical Antenna Feed.	20
Fig. 14	S-Band 3-Turn Helical Antenna with Feed Potted in RTV-60 Silicon Rubber Compound.	20

TABLES

Table I	Tip Field-Power Level Constant K.	11
Table II	Martian and Venusian Atmosphere Compositions Assumed for Tests	12

I INTRODUCTION

The antenna is a basic link in the exploration of space by man. Important to antenna operation in planetary atmospheres is power-handling capability and breakdown-power level. When the air or atmospheric gas surrounding an antenna breaks down, the performance of the antenna is changed radically: The VSWR is altered, the radiation pattern is distorted, the total radiated power is decreased, and the pulse shape is changed.

This study was primarily directed towards determining the power-handling capacity and breakdown-power level of typical antennas in simulated atmospheres for Mars and Venus. However, during the course of measurements, the simulated atmospheres for Mars and Venus were found to be similar to air in breakdown characteristics. It was therefore decided to complete the breakdown measurements in air.

A large part of this experimental investigation is an extension of measurements by Scharfman and Morita at Stanford Research Institute. Scharfman and Morita^{1*} considered the various physical mechanisms important in the breakdown process and the manner in which these mechanisms determine breakdown field strength. It was shown that for standard geometries--monopole, slot, parallel-plate, waveguide, coaxial transmission line, etc.--knowledge of the electric field strength and gas pressure is sufficient to predict breakdown-power level. This prediction should be acceptable for all geometries in which electric field strength can be related to power level.

*References are included at the end of this report.

II CYLINDRICAL MONOPOLE BREAKDOWN

A. BREAKDOWN IN AIR

Cylindrical monopole antennas used for breakdown measurements are illustrated in Fig. 1. Antenna tips are hemispherical of radius $d/2$. Breakdown measurements were made at 250 Mc, 1197 Mc, and 3000 Mc. Antenna length was 0.26λ at specified frequencies.

Antenna thickness coefficient, Ω , for cylindrical antennas is defined as

$$\Omega = 2 \ln \frac{4\ell}{d}$$

where

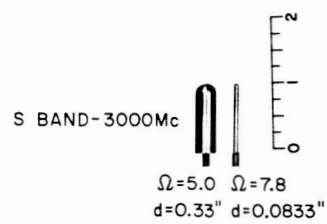
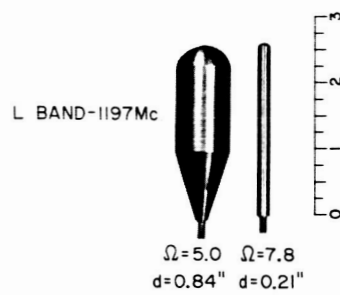
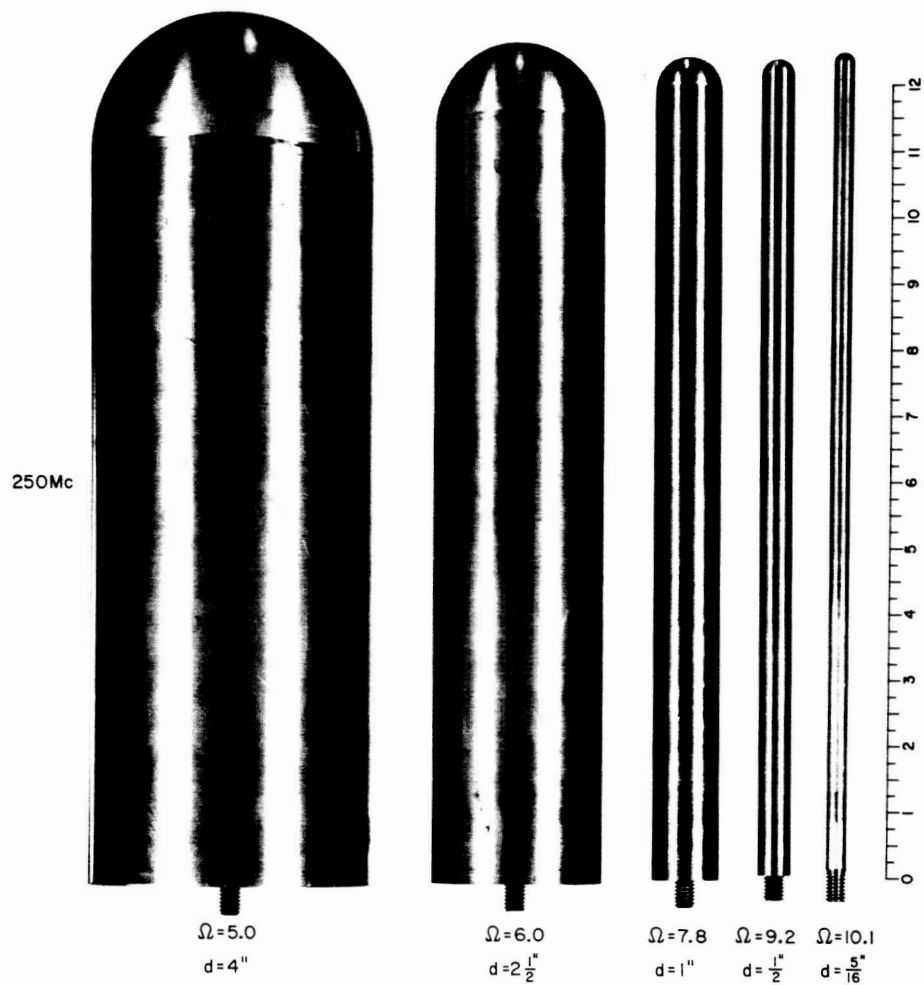
ℓ is the antenna length

d is the antenna diameter.

Measured power level at tip breakdown is plotted as a function of p/f (pressure/frequency) for eight monopole diameters in Fig. 2. The dashed-line curves were obtained from Reference 1. The greater power-handling capability of thick monopoles compared to thin ones is clearly indicated in Fig. 2. For the antennas considered here, the maximum electric field at the monopole tip surface will be approximately inversely proportional to the diameter, assuming a constant power is radiated.

Power to initiate breakdown (P , incident- P , reflected) for $p/f = 8 \times 10^{-4}$ mm Hg/Mc--representative of minimum breakdown power--is plotted in Figs. 3 and 4. In Fig. 3, breakdown power is plotted as a function d/λ . In Fig. 4, the solid curve represents breakdown power as a function of Ω . The dashed curve in Fig. 4 relates ℓ/d to Ω .

A $\Omega = 7.8$ cylindrical dipole antenna was constructed to operate at 1197 Mc. As expected, the power level at tip breakdown was twice that of the monopole.



P-4208-4

FIG. 1 MONOPOLE ANTENNAS

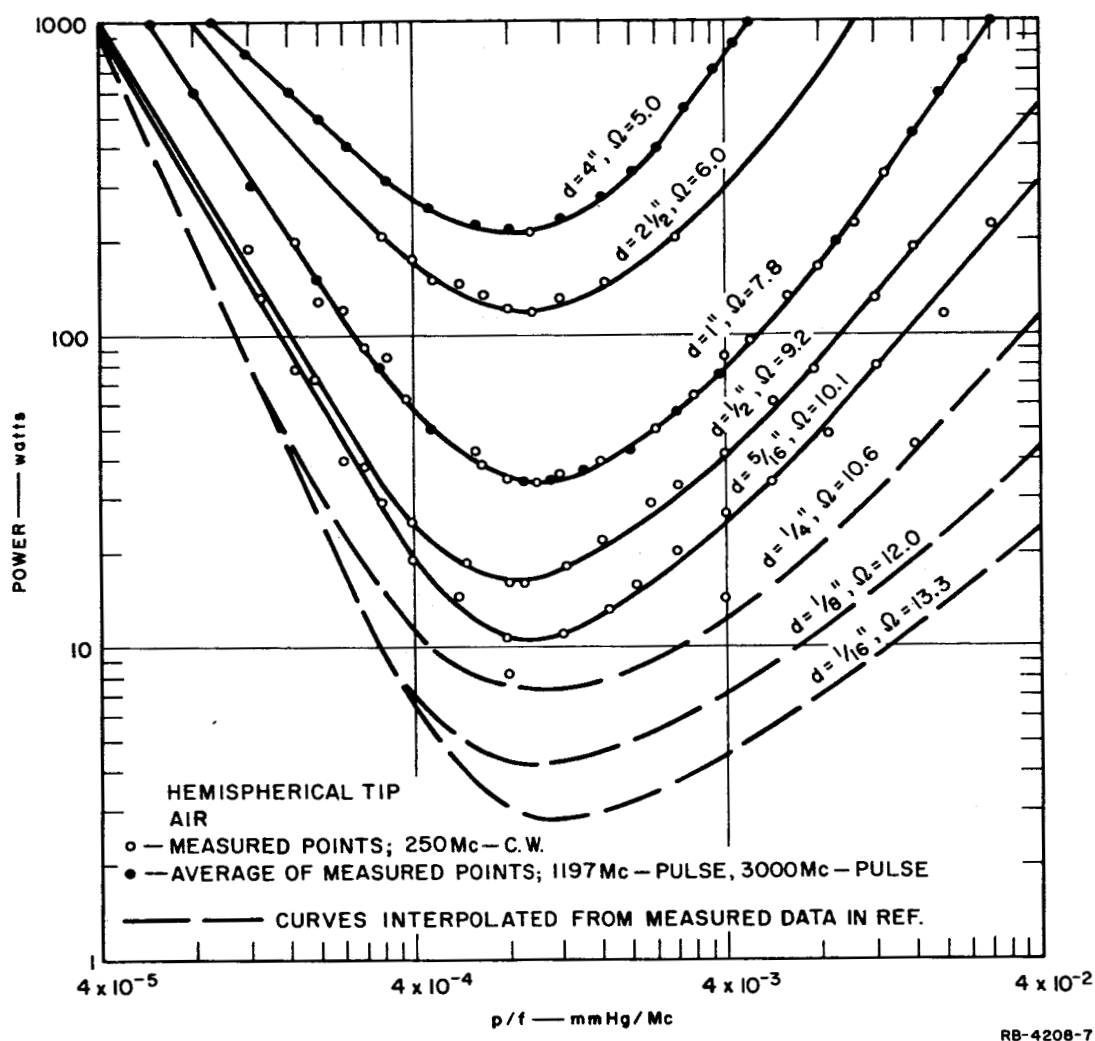
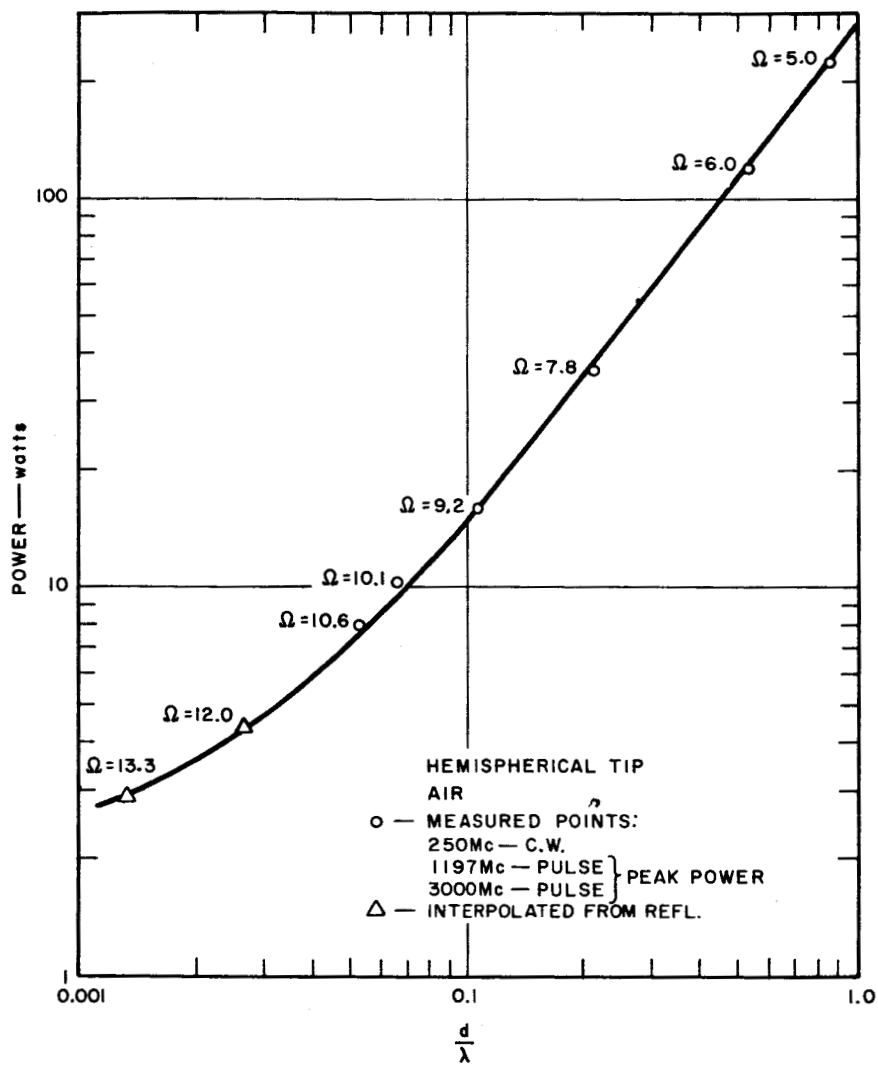


FIG. 2 POWER REQUIRED TO INITIATE BREAKDOWN IN AIR OF 0.26λ MONOPOLES AS A FUNCTION OF PRESSURE AND FREQUENCY

B. VERIFICATION OF ANTENNA SCALING PRINCIPLE

A study of the factors influencing the type of discharge under consideration here shows that for geometrically similar antennas, frequency scaling is applicable.² Aside from the usual electromagnetic similitude principle, it is required that

$$p\lambda(\text{or } \frac{p}{f}) = \text{constant}$$



RA-4208-8

FIG. 3 POWER REQUIRED TO INITIATE BREAKDOWN IN AIR OF 0.26λ MONOPOLES AS A FUNCTION OF DIAMETER AND FREQUENCY FOR $p/f = 8 \times 10^{-4}$ mmHg/megacycles

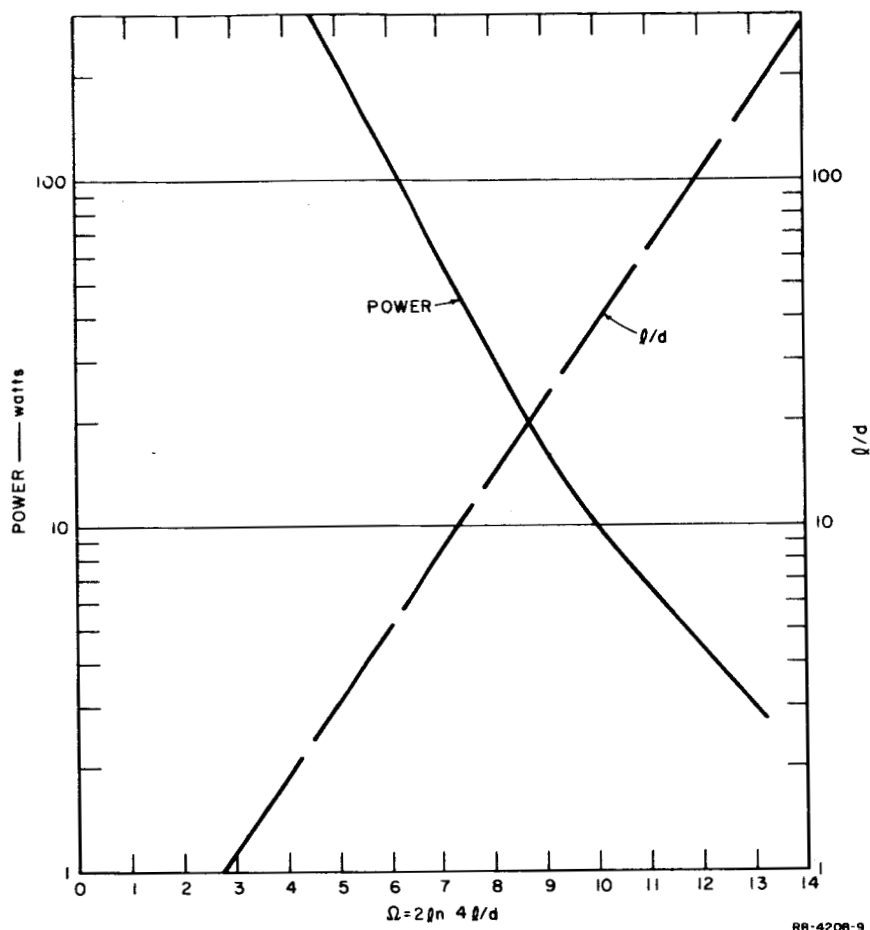


FIG. 4 POWER REQUIRED TO INITIATE BREAKDOWN IN AIR OF 0.26λ MONOPOLES AS A FUNCTION OF Ω AND l/d FOR $p/f = 8 \times 10^{-4}$ mmHg/megacycles

where

- p is the pressure
- λ is the wavelength
- f is the frequency.

The antenna scaling principle is verified in Figs. 5 and 6 for $\Omega = 7.8$ and $\Omega = 5$ monopoles at three frequencies: 250 Mc, 1197 Mc and 3000 Mc. Measured breakdown power level is plotted as a function of p/f . Power supplied at 250 Mc was CW; power supplied at 1197 Mc and 3000 Mc was pulsed.

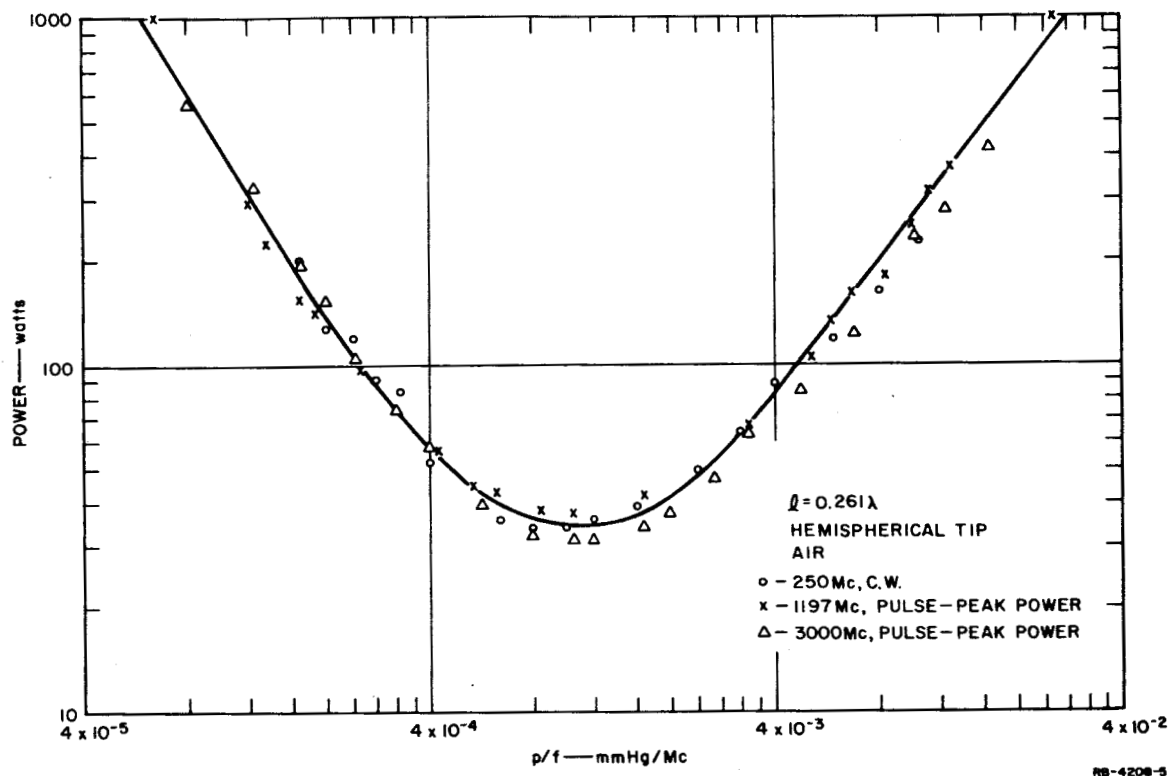


FIG. 5 VERIFICATION OF ANTENNA SCALING PRINCIPLE AND BREAKDOWN FOR $\Omega = 7.8$ MONOPOLES AS A FUNCTION OF PRESSURE AND FREQUENCY

In converting average power (meter reading) to peak power for pulse breakdown at 1197 Mc and 3000 Mc, an equivalent pulse width τ_e was required because magnetron pulses were not rectangular. Equivalent pulse width, τ_e , is defined as:

$$\tau_e = \frac{\int_{\tau_1}^{\tau_2} h(\tau) d\tau}{h_{\max}}$$

where

$h(\tau)$ is the pulse height as a function of width τ

h_{\max} is the maximum pulse height

τ_1 and τ_2 refer to time at the leading and trailing edges of the pulse.

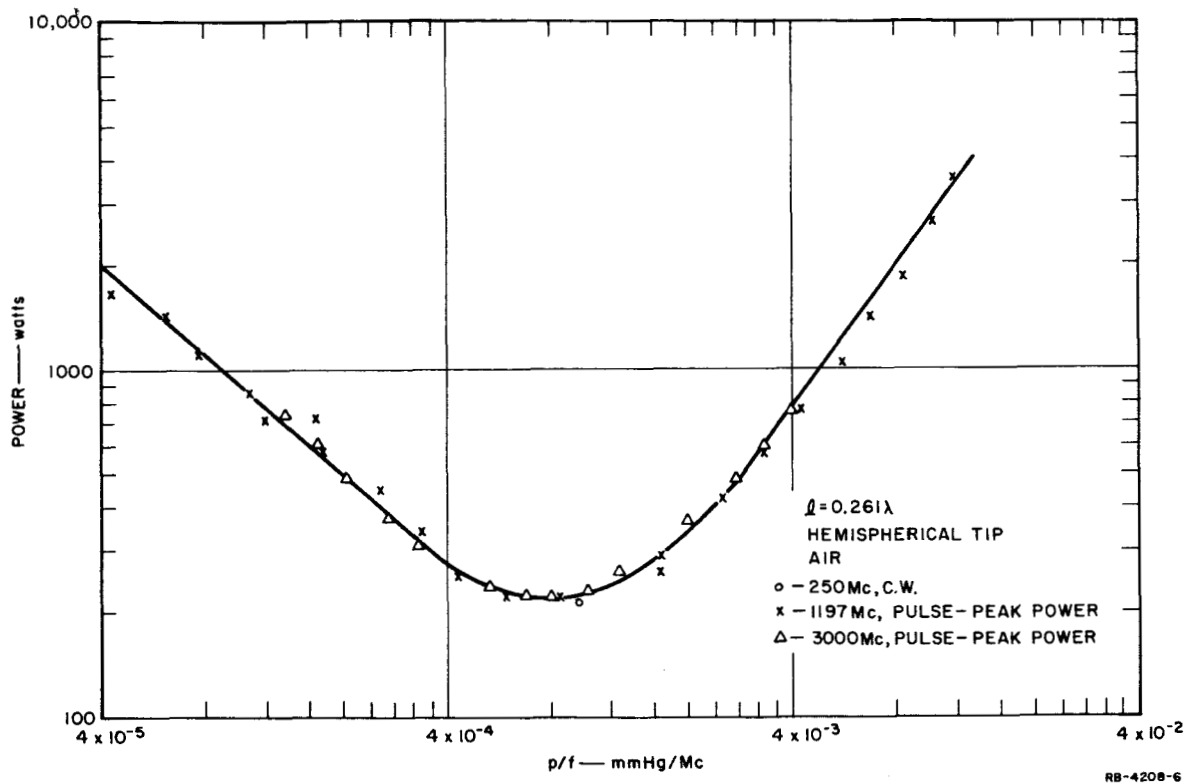


FIG. 6 VERIFICATION OF ANTENNA SCALING PRINCIPLE AND BREAKDOWN FOR $\Omega = 5.0$ MONOPOLES AS A FUNCTION OF PRESSURE AND FREQUENCY

Equivalent pulse width for breakdown measurements were computed as 5 μ sec at both 1197 Mc and 3000 Mc. Pulse repetition frequency was 200 pps at both 1197 Mc and 3000 Mc.

For pulse breakdown of monopole antennas, tip field and input power at breakdown are functions of pressure times pulsewidth--i.e., $p\tau$. As $p\tau$ increases, pulse breakdown level approaches the CW value and a function of pd . Pulse breakdown is discussed in detail in Reference 1. It is shown that for measurements presented in this report where $p\tau \gtrsim 10^{-6}$ mm Hg seconds and $pd \gtrsim 0.02$ mm Hg-cm peak power levels for pulse breakdown are approximately equivalent to power for CW breakdown. Figures 5 and 6 verify this equivalence.

C. BREAKDOWN FIELD MEASUREMENTS

For the monopole antenna considered here, the maximum field occurs at the tip which is the point at which breakdown takes place. The breakdown power level for the monopole is related to the tip field as follows:

$$P = K E_t^2$$

where

P = breakdown power level

K = Constant for a given antenna, determined by charge distribution

E_t = Electric field strength (rms volts) at the monopole tip.

The value of tip field required to initiate breakdown is determined by an effective field strength, E_e

$$E_e = \frac{E_t}{[1 + \omega^2/\nu_c^2]^{1/2}}$$

where

ω is the radian frequency of the applied power

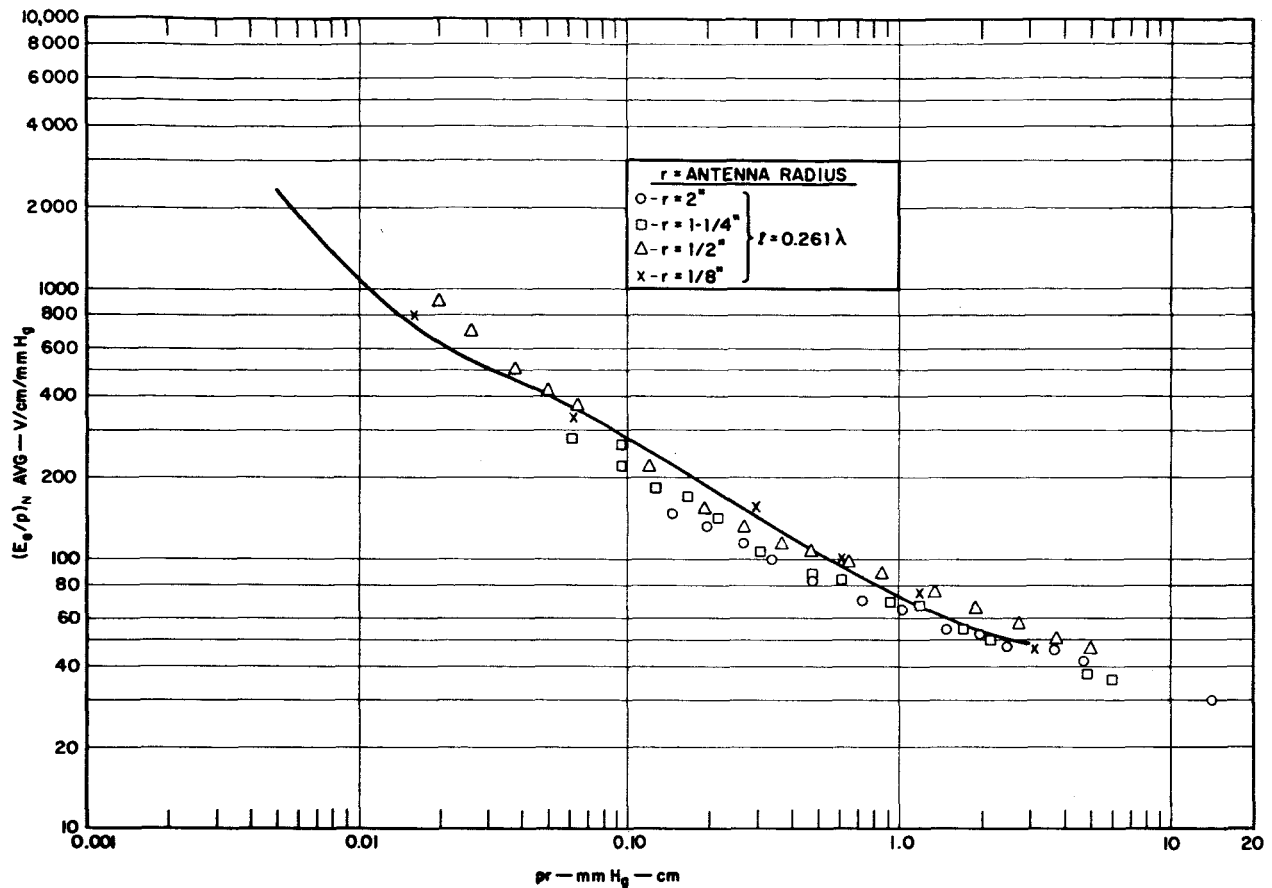
ν_c is the collision frequency in collisions per second.

In air, the collision frequency is assumed to be related to pressure by

$$\nu_c = 5.3 \times 10^9 p$$

where p is the pressure in mm Hg.

The effective field strength, E_e , required for breakdown is unique for a given field geometry and ambient pressure. Also, if the form of the near-zone field remains the same with some varying dimension (as with parallel plate transmission lines with varying spacing, narrow slot antennas with varying width, and monopoles with varying diameter), the value of E_e/p is a function of pressure p times the characteristic dimension. Normalized curves of E_e/p as a function of pr , where r is the monopole radius, can thus be used in predicting the breakdown power level of an antenna once E_t is related to the input power. A normalized E_e/p curve is presented in Fig. 7 and is independent of antenna height.



RB-2494-T-101

FIG. 7 AVERAGE VALUES OF NORMALIZED PARAMETERS FOR CW BREAKDOWN OF MONOPOLE ANTENNAS

The solid curve in Fig. 7 is reproduced from breakdown measurements by Scharfman and Morita¹ on 0.24λ monopoles of diameter $1/16''$, $1/8''$ and $1/4''$. Calibration of K for the solid curve was calculated* using the charge distribution for the $\Omega = 10$, quarter-wave antenna as presented by King.³

A direct measurement of E_t was made on the $1/4''$, $1''$, $2-1/2''$ and $4''$ hemispherically capped monopoles used in the 250-Mc breakdown tests. The measurement employed a small coaxial probe located at the tip of the

* See Ref. 1, Appendix A.

dipole. The data points plotted in Fig. 7 represent the tip field and breakdown power measurements on 0.26λ monopoles of diameter $1/4''$, $1''$, $2-1/2''$ and $4''$. As shown in Fig. 7 the measured data for thick antennas agrees well with previous field measurements on thin monopole antennas.

Calibration of K was made by direct measurement between parallel plates and by knowing that $E_e/p \rightarrow 30$ for large values of pr. The factor K is listed in Table I for the $1/4''$, $1''$, $2-1/2''$ and $4''$ monopoles.

TABLE I
TIPFIELD-POWER LEVEL CONSTANT K

$$P = K E_t^2$$

$$(\text{input power}) = K(\text{tip field})^2$$

Monopole Diameter, d	K for 0.26λ Monopoles
$1/4''$	0.000492
1 "	0.0142
$2-1/2''$	0.137
4 "	0.415

If the near-zone field about an antenna does not vary with varying characteristic dimension, E_e/p is no longer simply a function of pressure times the characteristic dimension. This occurs, for example, with slot antennas when the slot width becomes appreciable compared to a wavelength.

D. BREAKDOWN IN SIMULATED ATMOSPHERES FOR MARS AND VENUS

A brief survey of literature on the gas composition of the atmospheres of Mars and Venus has been conducted.⁴⁻¹¹ Data available for the atmosphere of Mars are more definitive than the data available for that of Venus. The data surveyed for the Martian atmosphere indicates that the neutral atmosphere is composed almost totally of nitrogen. Minor constituents of the Martian atmosphere are argon and carbon dioxide.

Spectroscopic observations indicate that the atmosphere of Venus has a larger quantity of carbon dioxide than the Martian atmosphere. Definitive models of the atmosphere of Venus cannot be obtained without penetrating the cloud cover surrounding the planet.

Breakdown tests have been made using volumetric gas compositions specified by JPL, which represent the expected extremes. These compositions are given in Table II.

TABLE II
MARTIAN AND VENUSIAN ATMOSPHERE COMPOSITIONS
ASSUMED FOR TESTS

<u>Mars</u>		
Carbon Dioxide	0.7%	7.2%
Argon	0.6%	6.0%
Nitrogen	98.7%	86.8%
<u>Venus</u>		
Carbon Dioxide	3%	25%
Argon	1%	1%
Nitrogen	96%	74%

The equipment used in creating the artificial atmospheres is shown in Fig. 8. It consists of a reservoir for mixing the various gases and a means of injecting each constituent separately. The correct gas mixture was obtained in the reservoir by using the Alphatron pressure gage and the method of partial pressures. Before each test the chamber was purged to remove the air and moisture with dry N₂, the principal

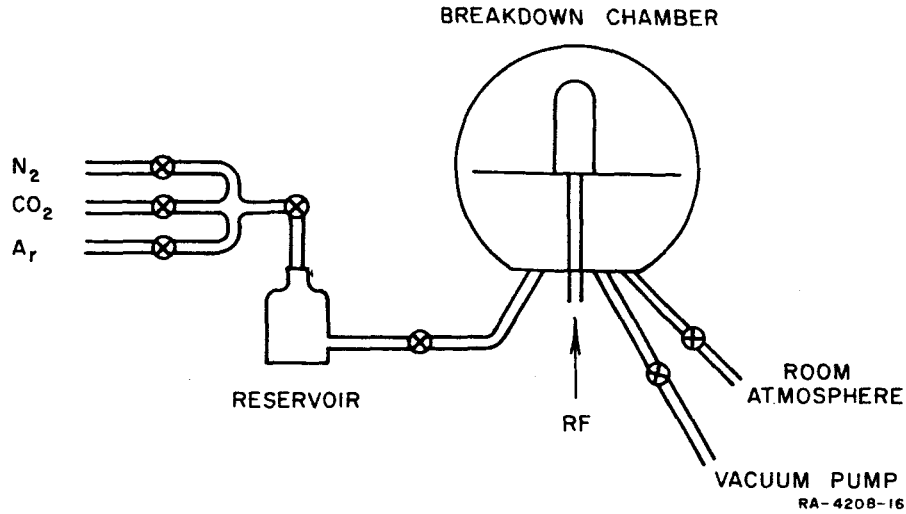


FIG. 8 GAS MIXING EQUIPMENT

constituent of the desired atmosphere. The chamber was then pumped well below the pressure where the measurement was to be made. Immediately prior to the measurement, the chamber pressure was increased to the desired level by transferring a portion of the gas mixture previously established in the reservoir. This method was employed so that any small leaks permitting air to enter the chamber would have a negligible affect.

Breakdown tests were performed on the 0.26λ monopole ($\Omega = 7.8$) at 250 Mc. Results are plotted in Fig. 9. It is readily seen that antenna breakdown in the simulated atmospheres does not differ from that in the earth's atmosphere-air.

One of the fundamental parameters in determining breakdown levels in a gas is the ionization rate (the number of ionizations per second per electron). Voltage breakdown of an antenna occurs when the gain in electron density due to ionization becomes equal to the loss of electrons by diffusion and attachment. Ionization rate in argon is higher than in air, in nitrogen, or in carbon dioxide. Ionization rate in air, in nitrogen, and in carbon dioxide are comparable within an order of magnitude. Thus small amounts of argon ($\leq 6\%$) in gas mixtures of air, nitrogen, and carbon dioxide do not significantly alter gas breakdown

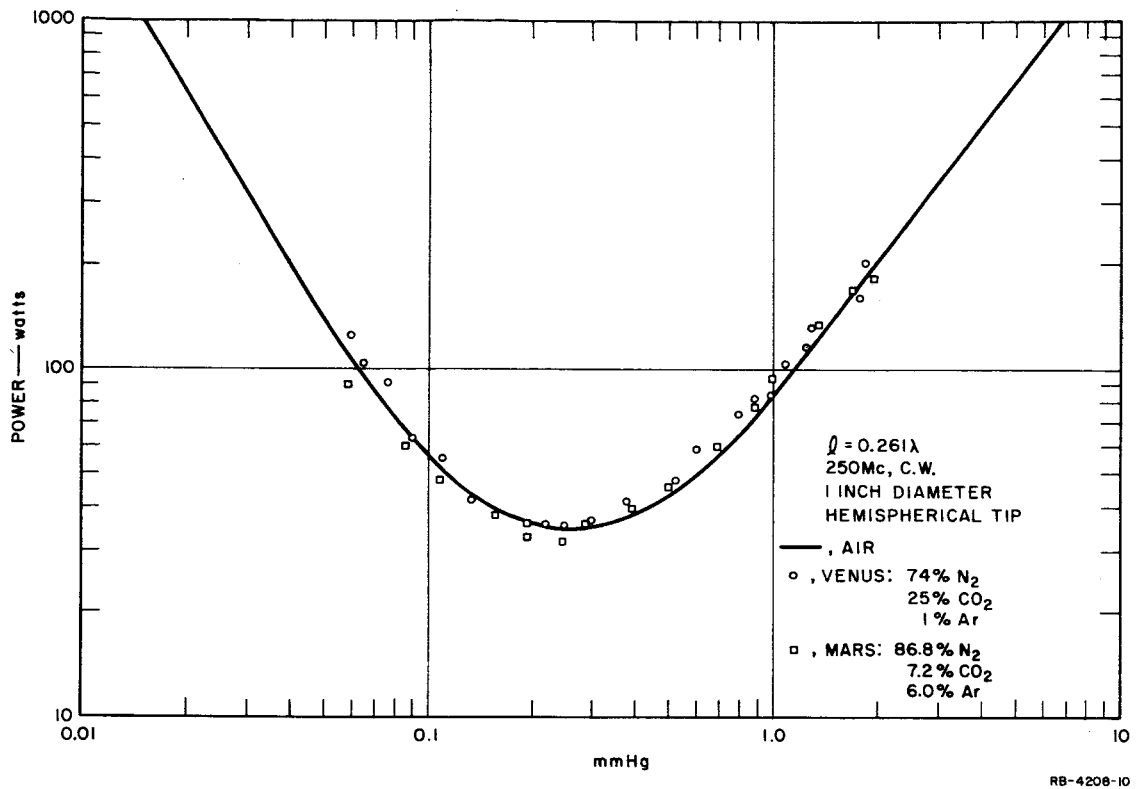


FIG. 9 MEASURED VALUES OF POWER TO INITIATE CW BREAKDOWN OF A $\Omega = 7.8$ MONOPOLE IN SIMULATED ATMOSPHERES OF MARS AND VENUS

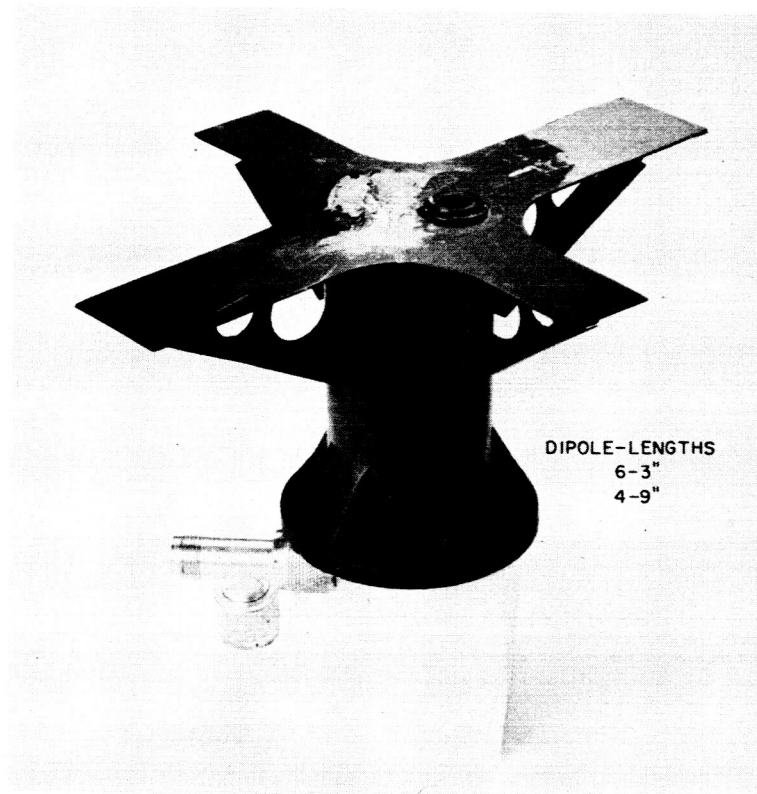
characteristics as indicated in this study. The percentage of argon at which breakdown characteristics change significantly has not been evaluated in this study.

III CROSS-DIPOLE ANTENNA BREAKDOWN

Breakdown tests were made in air on a cross-dipole antenna at 890 Mc and 1197 Mc. The antenna shown in Fig. 9 and supplied by JPL is circularly-polarized at 890 Mc. Polarization characteristics are unknown at 1197 Mc. Dipole total lengths were 4.9 in and 6.3 in.

With available power of 10 watts at 890 Mc fed into the array no breakdown occurred.

Peak pulse power required to initiate breakdown at 1197 Mc is plotted in Fig. 10 as a function of pressure. Equivalent pulse width was 5.0 μ sec and PRF was 200 pps. Breakdown occurred at the feed for all measurements. Since breakdown occurs at the feed, where the VSWR was less than 2:1, the power levels measured at 1197 Mc are indicated of the feed breakdown power level at 890 Mc.



CROSSED-DIPOLE ANTENNA

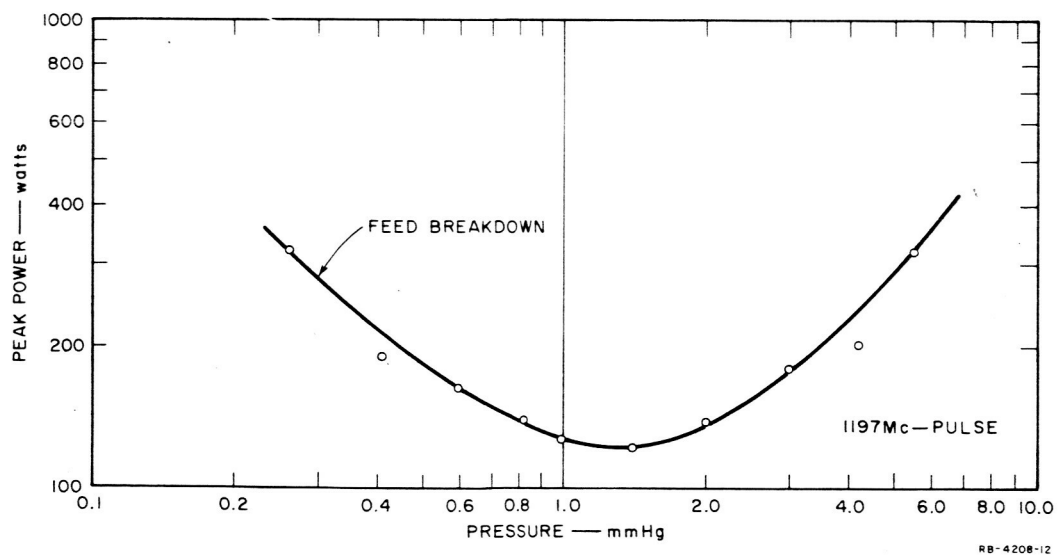


FIG. 10 POWER REQUIRED TO INITIATE BREAKDOWN IN AIR OF A CROSSED-DIPOLE ANTENNA

IV HELICAL ANTENNA BREAKDOWN

Peak pulse power to initiate breakdown was measured for scaled helical antennas at 1197 Mc and 3000 Mc. Pulse width was 5 μ sec at 1197 Mc, and PRF was 200 pps at both frequencies. A photograph of the 6-turn, L-band helix used in the measurements is presented in Fig. 11.

Design data and breakdown measurements on 6-turn, axial-mode helical antennas are presented in Fig. 12. Breakdown occurred at the coaxial feed where field is a maximum.

The dashed curves in Fig. 12 are theoretical predictions for breakdown at the helical feed. Referring to Fig. 13, the helical feed is a 50-ohm tapered coaxial transition from a RG-8 U cable to the helical element. Breakdown power level for the feed is predicted by

$$P = \frac{[d/b (b/a)]^2 [1 + \omega^2 / \nu_c^2]}{R} E_e^2 .$$

Parameters, a , a/b , and R are defined in Fig. 12. Dimension b was assumed to be 0.745 in for calculating the breakdown power. The ratio d/b is simply an approximation to the ratio of the electric field at distances $d/2$ and $b/2$ from the center of the feed. Parameters ω , ν_c and E_e have been defined earlier. In calculating P , E_e/p was obtained at specific pd's from coaxial line breakdown data in Reference 1.

Breakdown measurements were made on L-band, 3-turn and 1-1/2-turn helices of design similar to the 6-turn helix. Breakdown level was unchanged relative to the 6-turn helix and occurred at the helical feed.

Breakdown measurements were made also on S-band, 3-turn and 6-turn helices with a potting of RTV-60° silicon rubber compound at the feed. The 3-turn helix and potting is illustrated in Fig. 14. Minimum breakdown power for the two antennas was 660 watts at 3 mm Hg. Referring to Fig. 11, the increase in feed power handling capability with potting is 6.5 db.

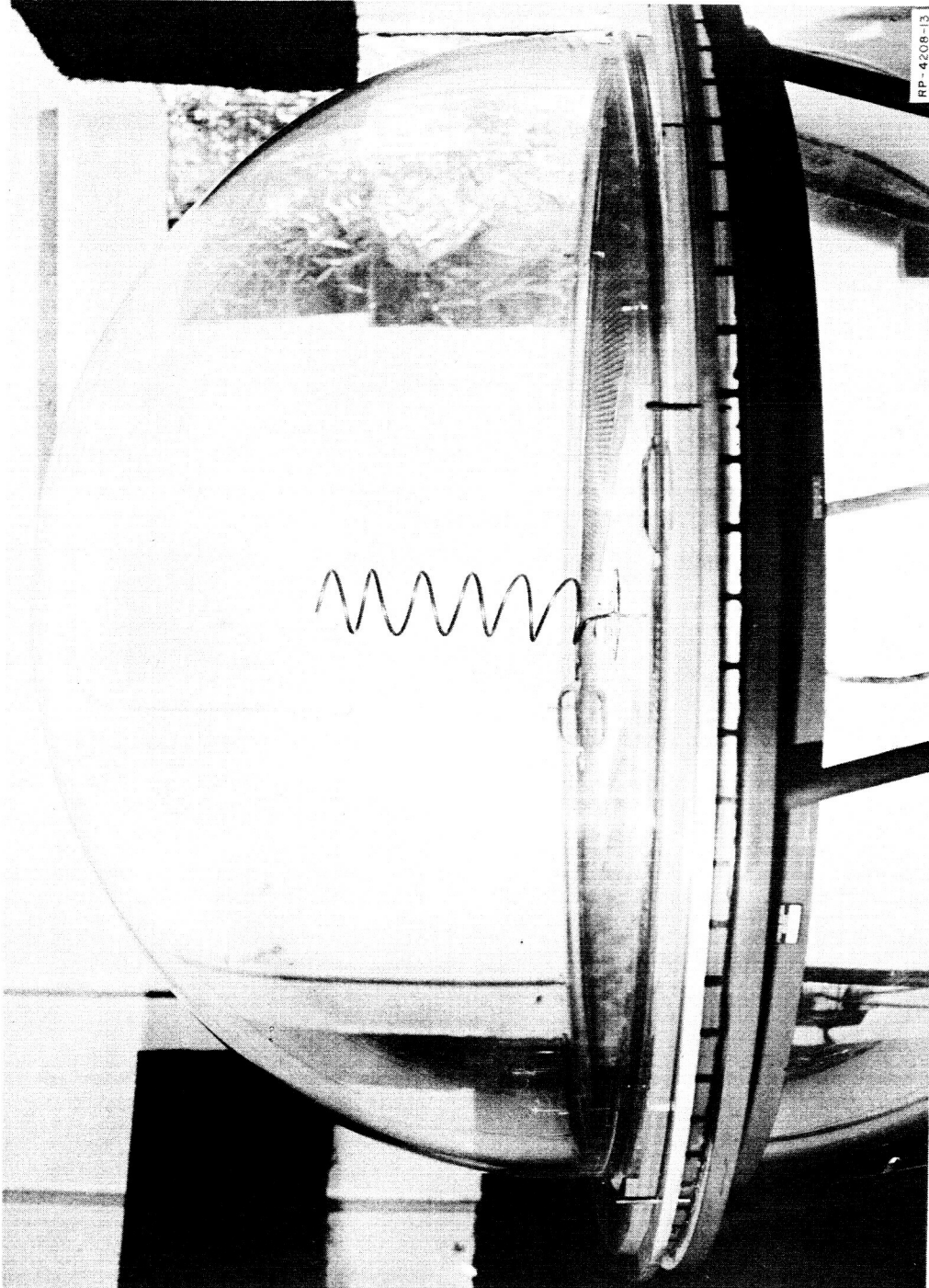
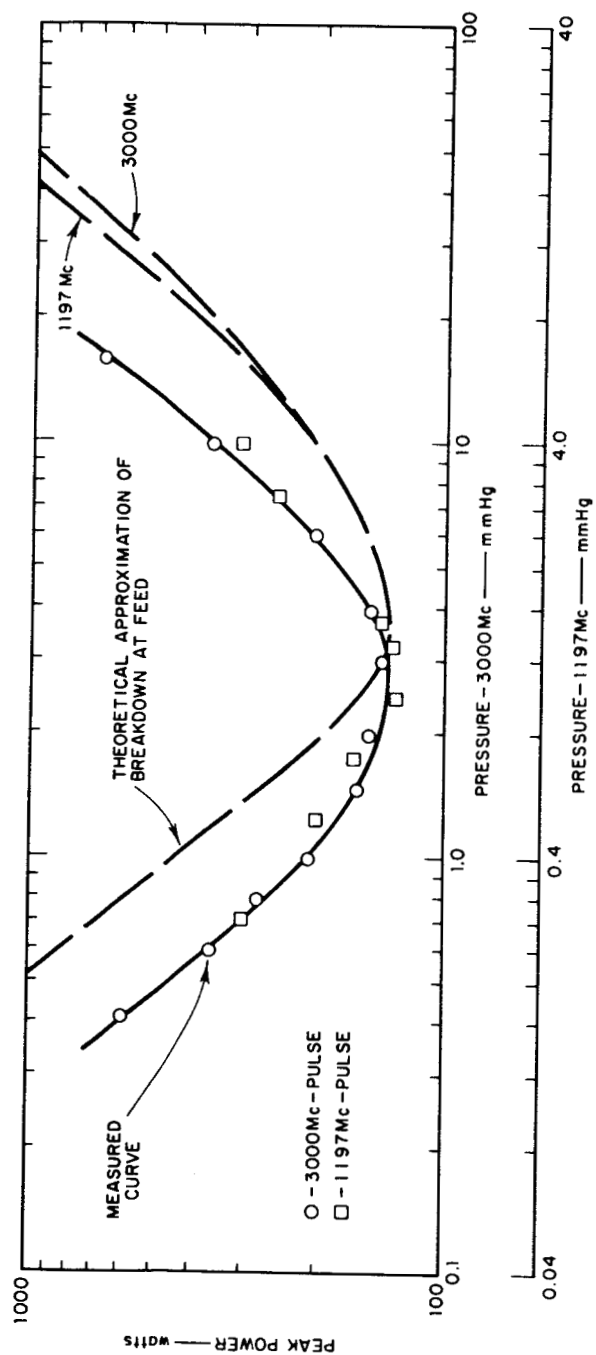
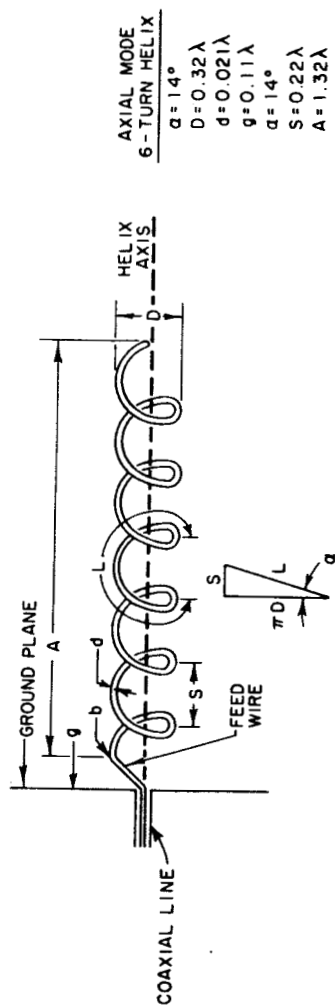


FIG. 11 L-BAND 6-TURN HELICAL ANTENNA IN PLEXIGLAS CHAMBER



RB-4208-11

FIG. 12 POWER REQUIRED TO INITIATE BREAKDOWN IN AIR OF 6-TURN
AXIAL-MODE HELICAL ANTENNA

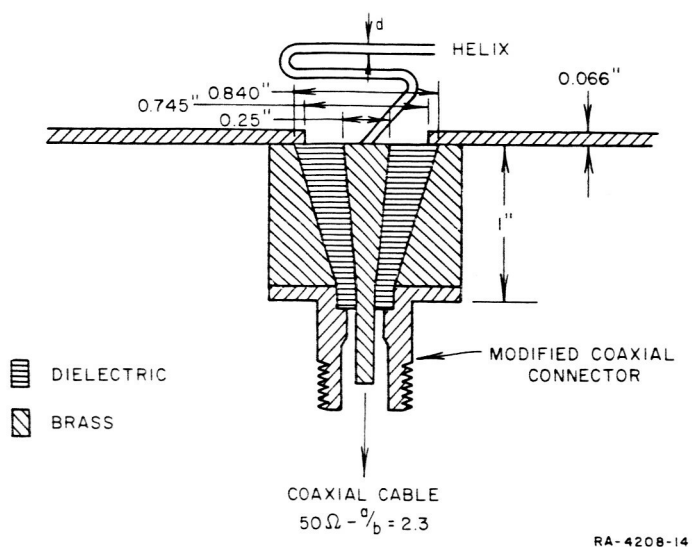
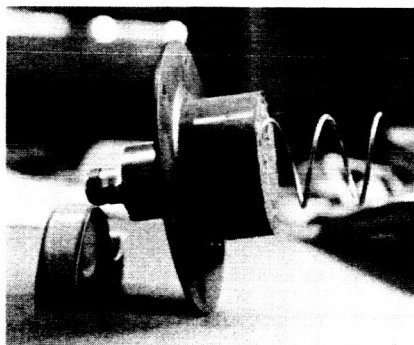


FIG. 13 HELICAL ANTENNA FEED



CYLINDRICAL POTTING
 $1\frac{3}{16}$ " HIGH
 $2\frac{1}{4}$ " DIAMETER

RA-4208-15

FIG. 14 S-BAND 3-TURN HELICAL ANTENNA WITH
 FEED POTTED IN RTV-60 SILICON RUBBER
 COMPOUND

V CONCLUSIONS

- (1) Breakdown of antennas in the simulated atmospheres of Venus and Mars specified by JPL does not significantly alter the breakdown experienced in air.
- (2) Power-handling capability of cylindrical antennas increases as Ω increases and in a manner one would predict on the basis of knowing the electric field configuration.
- (3) Breakdown power of monopole antennas can be predicted from normalized E_e/p curves, where the correspondence between the input power level and peak electric field intensity can be established.

REFERENCES

1. W. E. Scharfman and T. Morita, "Voltage Breakdown of Antennas at High Altitudes," Technical Report 69, SRI Project 2494, Contract AF 19(604)-3458, Stanford Research Institute, Menlo Park, California (April 1960).
2. H. Margenau, "Theory of High Frequency Discharges, IV Note on the Similarity Principle," Phys. Rev. 73, 4, p. 326 (February 15, 1958).
3. R. W. P. King, The Theory of Linear Antennas, Chapter II (Harvard University Press, Cambridge, Massachusetts, 1956).
4. F. I. Ordway III, Editor, Advances in Space Science and Technology, Parts 2 and 3 (Academic Press, New York and London, 1961).
5. W. W. Kellogg and Carl Sagan, "The Atmospheres of Mars and Venus," A Report of the Ad Hoc Panel on Planetary Atmospheres of the Space Science Board, Publication 944, National Academy of Sciences, National Research Council, Washington, D.C. (1961).
6. J. H. Shaw and N. T. Bobrovnikoff, "Natural Environment of the Planet Venus," WADC Phase Technical Note 847-2 (February 1959), AD 242 176.
7. "Atmosphere of Mars, Review of Soviet Literature," AID Report 61-138 Science and Technology Section, Aerospace Information Division, ASTIA (October 1961), AD 266 481.
8. M. H. Briggs, "The Chemistry of Mars--1. The Atmosphere," Journal of the British Interplanetary Society, Vol. 17, No. 11, pp. 391-393 (September-October 1960).
9. G. F. Schilling, "A Note on the Atmosphere of Mars," Journal of Geophysical Research, Vol. 67, No. 3, pp. 1170-1172 (March 1962).
10. C. C. Klieis, C. H. Carliss, and H. F. Kiess, "Evidence for Oxides of Nitrogen in the Atmosphere of Mars," Science, Vol. 131, p. 1319 (29 April 1960).
11. A. D. Danitov, "Model of Venus and Mars Ionospheres," 5th COSPAR Meeting, Washington, D.C. (1962).

ACKNOWLEDGEMENT

The authors wish to acknowledge the assistance of Mr. W. E. Scharfman and Dr. Tetsu Morita during this effort. Mr. R. J. Mora assisted in the construction of models and in the breakdown measurements.

STANFORD
RESEARCH
INSTITUTE

MENLO PARK
CALIFORNIA

Regional Offices and Laboratories

Southern California Laboratories
820 Mission Street
South Pasadena, California

Washington Office
808 17th Street, N.W.
Washington 5, D.C.

New York Office
270 Park Avenue, Room 1770
New York 17, New York

Detroit Office
The Stevens Building
1025 East Maple Road
Birmingham, Michigan

European Office
Pelikanstrasse 37
Zurich 1, Switzerland

Japan Office
911 Iino Building
22, 2-chome, Uchisaiwai-cho, Chiyoda-ku
Tokyo, Japan

Representatives

Honolulu, Hawaii
Finance Factors Building
195 South King Street
Honolulu, Hawaii

London, England
19 Upper Brook Street
London, W. 1, England

Milan, Italy
Via Macedonio Melloni 40
Milano, Italy

London, Ontario, Canada
P.O. Box 782
London, Ontario, Canada